Appl. Phys. A 75, 89–99 (2002) / Digital Object Identifier (DOI) 10.1007/s003390101058

Applied Physics A
Materials
Science & Processing

III−V compound semiconductor (001) surfaces

W.G. Schmidt*

Computational Materials Science Group, Institut für Festkörpertheorie und Theoretische Optik, Friedrich-Schiller-Universität, Max-Wien-Platz 1, 07743 Jena, Germany

Received: 18 May 2001/Revised version: 23 July 2001/Published online: 3 April 2002 –

Abstract. There has been renewed interest in the structure of III−V compound semiconductor (001) surfaces caused by recent experimental and theoretical findings, which indicate that geometries different from the seemingly well-established dimer models describe the surface ground state for specific preparation conditions. I review briefly the structure information available on the (001) surfaces of GaP, InP, GaAs and InAs. These data are complemented with first-principles total-energy calculations. The calculated surface phase diagrams are used to explain the experimental data and reveal that the stability of specific surface structures depends largely on the relative size of the surface constituents. Several structural models for the Ga-rich GaAs (001)(4×6) surface are discussed, but dismissed on energetic grounds. I discuss in some detail the electronic properties of the recently proposed cation-rich GaAs (001)ζ(4×2) geometry.

PACS: 68.35.Bs; 68.35.Md; 73.20.At

The (001)-oriented substrates of III−V semiconductors are commonly used in growth technologies like molecular beam epitaxy (MBE) or metal-organic vapour phase epitaxy (MOVPE). Apart from this application aspect, much interest in the structure and stability of the (001) surfaces has also been caused by the rich variety of surface reconstructions which can be observed depending on the surface preparation. For instance the GaAs (001) surface shows a $c(4\times4)$ symmetry for As-rich conditions, but changes its periodicity to $(2\times4)/c(2\times8)$ and finally $(4\times2)/c(8\times2)$ as the surface gets more cation-rich. In addition, a large variety of transient structures or apparent symmetries such as (2×3), (2×1), (3×1), (3×6), (2×6), (6×6), (4×6), etc., are reported [1–4].

The large number of surface structures observed on III−V(001) surfaces have early on prompted attempts to classify and understand them from a more general point of view. For example a so-called electron-counting rule (ECR) was recognised to govern many reconstructions [5]. A surface structure satisfies this model if it is possible to have all the dangling bonds on the electronegative element occupied and all the dangling bonds on the electropositive element empty, given the number of available electrons. This condition results necessarily in there being no net surface charge. The ECR together with the dimerisation as the major mechanism to reduce the number of dangling bonds on III−V (001) surfaces were able to explain successfully a large number of surface geometries. This success prompted Mönch to write [2]: "The electronic energy of such surfaces will be lowest when i. surface atoms in the top layer are forming dimers and ii. dangling bonds are filled on surface anions and are empty at the surface cations".

While the ECR gives an indication of which structures might be stable and which should not be, it does not allow us to discriminate energetically between two structures complying with the electron-counting principle. A major progress in that respect was the work by Northrup and Froyen on the role of electrostatic interactions between the surface structural units [6]. They showed that Coulomb repulsion between negatively charged anion dimers favours the two-dimer $\beta2(2\times4)$ structure over the three-dimer $\beta(2\times4)$ structure for GaAs. Based on similar electrostatic arguments, Schmidt et al. [7] predicted recently that a one-dimer $\alpha2(2\times4)$ structure should be lower in energy than the hitherto accepted $\alpha(2\times4)$ model.

The estimation of relative surface energies from empirical concepts was further refined by Zhang and Zunger [8], who observed that the large collection of equilibrium surface structures is built from a limited number of recurring local structural motifs, such as threefold-coordinated pyramidal anions or surface dimers. The energies of these structural motifs can be obtained from a fit to the results of ab initio calculations on flat surfaces and bulk defects. Based on motif energies obtained in such a way, Zhang and Zunger estimated the surface energies for reconstructions larger than what could be dealt with from first principles at that time. The accuracy of their method is limited, however, as I will show below, using the GaAs (001)(2×6) surface as an example.

A related approach has been followed by Mirbt et al. [9]. Starting from atomic energy levels and bonding energies they derived a very simple expression called a surface reconstruc-

*(Fax: +49-3641/947152; E-mail: w.g.schmidt@ifto.physik.uni-jena.de)

tion parameter in order to assess the stability of reconstruction models. According to this parameter, for the stability of III−V surfaces it is required that under cation-rich conditions the sum of anion dangling bonds and anion–anion bonds should be minimised. For anion-rich conditions the expression $N_a - N_{a-a} + 2N_{c-c}$ needs to be minimised, where N_a is the number of anion dangling bonds and N_{a-a} and N_{c-c} denote the numbers of anion–anion and cation–cation bonds. Later, the same group pointed out how local stress may modify these rules [10].

The GaAs dimer models were extrapolated and used to explain the (001) surface geometries of materials like GaP, InP and InAs. In many cases these dimer geometries allowed us indeed to explain the experimental findings and a consistent picture seemed to emerge [3]. In the last three to four years, however, it became more and more clear that our understanding of III−V (001) surface reconstructions is still far from being complete and that the complexity of the forces driving the formation of certain reconstructions is not captured alone by the simple rules given above. Symmetric dimers, for example, fail to explain all (001) surface structures, as became obvious from the scanning tunnelling microscopy (STM) images of the In-rich InP (001)(2×4) surface [11]. Mixed hetero-dimers consisting of anions and cations were proposed instead for cation-rich surfaces of InP [12] and GaP [13]. Moreover, (2×1) and (2×2) reconstructions were found for P-rich InP surfaces [14], while a (2×1) surface was reported for GaP (001) [15]. It is known, however, that the (2×4) reconstruction is the smallest unit cell which complies with the ECR [5]. Violations of the electron-counting rule were also reported for AlSb and GaSb (001) surfaces [16]. The GaAs (001) surface is arguably the most intensively investigated compound semiconductor surface. Its stoichiometry-dependent surface structure seemed to be well-established from both experiment and theory. Nevertheless, even for GaAs, recent theoretical work questions the validity of the 'traditional' dimer model to explain the cation-rich $(4 \times 2)/c(8 \times 2)$ reconstruction [17].

In the present paper I will briefly review the experimental and theoretical findings on the structure of the (001) surfaces of GaP, InP, GaAs and InAs. These findings are explained and put in perspective using surface phase diagrams derived from first-principles total-energy calculations. The calculations presented here are well-converged and on the same footing for all materials considered. They can thus be used to identify chemical trends.

1 Method

Density-functional theory [18, 19] in the local-density approximation [20, 21] (DFT–LDA) together with nonlocal norm-conserving pseudopotentials [22] is used to determine the structurally relaxed ground states of the surface structures. The Ga $3d$ and In $4d$ electrons, respectively, are partially taken into account by means of a nonlinear core correction to the exchange and correlation energies. A massively parallel, real-space finite-difference method [23] is used to deal efficiently with the large unit cells needed to describe the surface. A multigrid technique is employed for convergence acceleration. The spacing of the finest grid used to represent the electronic wave functions and the charge density was determined through a series of bulk calculations. We find that structural and electronic properties are converged for a spacing corresponding to 4% of the bulk lattice constant. The calculations were performed using the theoretical equilibrium lattice constants of 5.39, 5.84, 5.57 and 6.00 Å, respectively, for GaP, InP, GaAs and InAs. They are slightly smaller than the corresponding experimental values measured at room temperature (5.45, 5.87, 5.65 and 6.06 Å [24]) due to the overestimation of the bond strengths typical for LDA calculations and the neglect of temperature effects.

The surfaces are modelled by using periodic supercells. They contain material slabs about 12 Å thick, separated by 12 Å of vacuum. The surface dangling bonds at the bottom layer are saturated with fractionally charged pseudohydrogens. The investigated geometries were relaxed until all calculated forces were below 20 meV/Å. The atoms in the lowest bilayer were kept frozen in the ideal bulk configuration. Integrations in the surface Brillouin zone are performed over four special $\boldsymbol{k}$ points in its irreducible part.

In order to compare energetically surface structures representing different stoichiometries, one has to take into account the chemical potentials μ of the surface constituents. Since the surface is in equilibrium with the bulk material, they are related to each other: their sum equals the chemical potential of the bulk semiconductor. Consequently, the surface formation energy may be written as a function of a single variable, which I take to be the relative chemical potential of the cation with respect to its bulk phase, $\Delta\mu$ (Ga, In). The computational accuracy in determining the chemical potentials is of the order of 0.1 eV [25]. The uncertainty of the calculated surface energies is less than 0.01 eV per surface atom.

2 Results and discussion

2.1 GaP

Experimentally, (4×2) [15, 26–32] , (2×4) [13, 26, 33–38], $(2 \times 1)/(2 \times 2)$ [13, 33, 37, 38] and (4×4) reconstructions [35] were observed for GaP (001) surfaces with increasing P content. First-principles total-energy calculations confirmed the stability of (2×4) [10, 13] and $c(4 \times 4)$ reconstructions [39]. They gave no indication, however, for a (4×2) symmetry. Recent experimental studies [13, 37] also suggest that the reported (4×2) periodicities are in fact (2×4) reconstructions, provided the crystal axes are defined according to the usual notation. The wrong symmetry assignment was probably caused by the fact that cation-rich GaAs (001) surfaces, often serving as a model case, reconstruct (4×2).

Pulci et al. [40] calculated the surface energy for a large variety of structures put forward to explain the GaP $(2 \times 1)/(2 \times 2)$ surfaces observed for P-rich preparation conditions. The surface phase diagram for GaP shown in Fig. 1 contains the energetically most favourable $(2 \times 1)/(2 \times 2)$ reconstructions as found by Pulci et al. [40] in conjunction with earlier total-energy results by Schmidt and co-workers [13, 39]. The corresponding equilibrium structures are shown in Fig. 2.

The calculated phase diagram predicts two (2×4) reconstructed surface structures which should occur for Ga-

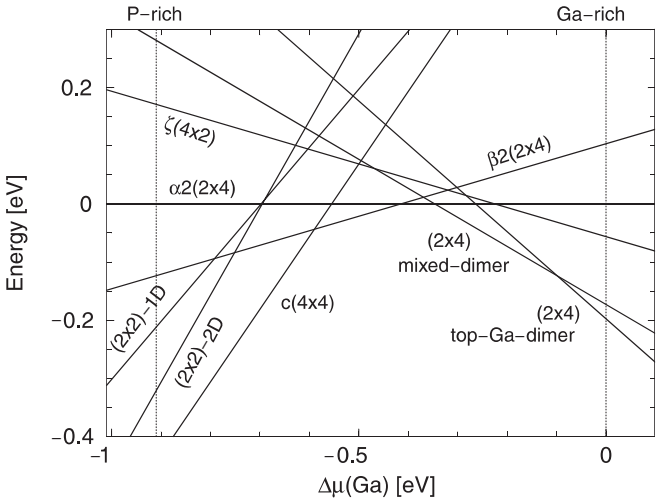

Fig. 1. Relative formation energy per (1×1) unit cell for GaP surface reconstructions vs. the cation chemical potential. *Dashed lines* mark the approximate anion- and cation-rich limits of the thermodynamically allowed range of $\Delta\mu$ (Ga)

rich preparation conditions, the top-Ga-dimer model and the mixed-dimer model. For surfaces with a balanced stoichiometry the $\alpha 2(2 \times 4)$ geometry has the lowest energy, whereas in somewhat more P-rich conditions the $\beta 2(2 \times 4)$ surface will form. An even higher supply of P should finally lead to a $c(4 \times 4)$ surface as known from As-rich GaAs surfaces. Smaller reconstructions, such as (2×1) and (2×2), are unstable.

At least two different (2×4) phases could also be discriminated by means of reflectance anisotropy spectroscopy (RAS) [13, 36, 37]. The comparison of the measured RAS data with the calculated spectra [39, 41] gives strong evidence that the mixed-dimer structure corresponds to the Ga-rich phase of GaP (001)(2×4). This assignment is corroborated by the recently measured surface core-level shifts [33]: two surface Ga components were assigned to three-fold-coordinated Ga atoms and Ga−Ga bonds. These two components can be explained both by the top-Ga-dimer structure and the mixed-dimer model. Only the latter, however, explains the measured surface P component, supposed to arise from three-fold-coordinated P atoms. This indicates that the extreme Ga-rich limit, which according to the total-energy calculations [13, 39] is characterised by the top-Ga-dimer model, may actually not be reached experimentally. That was recently supported by a comparison of simulated and measured STM images for GaP (001) surfaces [42]. The measured RAS data [13, 36, 37] further indicate that the more P-rich (2×4) reconstructions feature P−P dimers oriented along $[1\bar{1}0]$ and the breaking of [110]-oriented Ga−Ga bonds. The respective fingerprints in the optical spectra are very well described by theoretical calculations for the $\alpha 2(2 \times 4)$ and the $\beta 2(2 \times 4)$ models [39, 41]. The microscopic surface structure of the (2×4) reconstructed surface thus seems well understood. A detailed account of its electronic structure is given in [39].

The surface structures for higher P contents are not completely understood. Experimentally a $(2 \times 1)/(2 \times 2)$ reconstruction is observed which has been tentatively attributed to the surface termination by either P−P dimers [13, 15, 37, 43] or mixed Ga−P dimers [33]. Pulci et al. [40] investigated a large number of plausible (2×1) and (2×2) geometries. The energetically most favourable structures are the formation of one $((2 \times 2)$-1D) or two $((2 \times 2)$-2D) P−P dimers on top of a completely P-covered GaP (001)(2×2) surface. From the surface phase diagram in Fig. 1 it is obvious, however, that the $c(4 \times 4)$ reconstructed GaP surface is substantially lower in energy than the (2×2) surface. I am aware of only one experimental study reporting a (4×4) surface [35]. The failure of the calculations to explain the experimental data satisfactorily may indicate that the formation of the $c(4 \times 4)$ structure is kinetically limited, i.e. the observed $(2 \times 1)/(2 \times 2)$ symmetry does not correspond to an equilibrium structure. The calculations may also simply have missed a structure. On the other hand, the experimental observation of a $(2 \times 1)/(2 \times 2)$ surface could be an artefact of remaining adsorbates such as hydrogen related to the surface-preparation procedures.

2.2 InP

Similarly to the case of GaP, the cation-rich InP (001) surface was first reported to exhibit a (4×2) reconstruction [44–51]. This conclusion was most likely reached by assuming a dir-

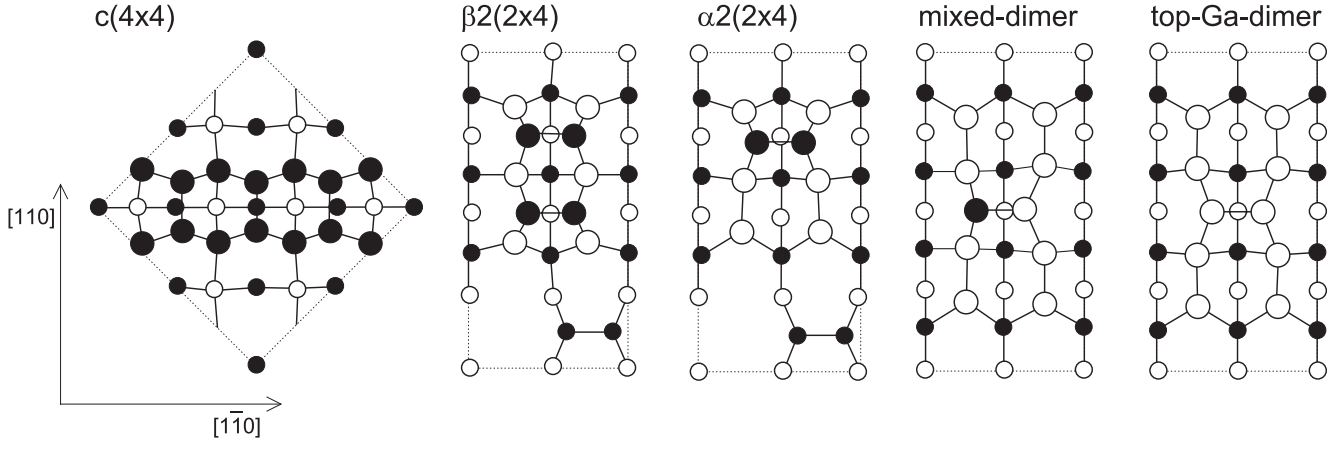

Fig. 2. Top view of relaxed GaP (001) surface structures, ordered according to the Ga coverage. *Empty* (*filled*) *circles* represent Ga (P) atoms. Positions in the uppermost two atomic layers are indicated by *larger symbols*

ect analogy to the cation-rich GaAs surface. There is now a consensus, however, that the In-rich InP (001) surface is in fact (2×4) reconstructed [11, 14, 52–67]. That is in accord with first-principles calculations on InP (001) [9, 12, 68]. For more P-rich surfaces, $(2 \times 1)/(2 \times 2)$ reconstructions are observed [14, 52, 59–62, 65, 66, 69, 70] while the most P-rich surfaces seem to be $c(4 \times 4)$ reconstructed [14, 59, 61].

In Fig. 3 the calculated phase diagram of InP (001) surfaces is shown. The corresponding ground-state geometries are given in Fig. 4. For In-rich, stoichiometric and slightly P-rich ($\Theta = 0.75$) surfaces, (2×4) reconstructed mixed-dimer, $\alpha 2$ and $\beta 2$ geometries, respectively, are predicted. For even more P-rich surfaces, (2×2) and $c(4 \times 4)$ reconstructions should occur. These symmetries agree with the experimental observations discussed above.

In particular, the structure of the In-rich (2×4) surface, the formation of mixed In−P dimers on top of a cation-terminated substrate, suggested by the present author and others in 1998 [12], is meanwhile well established. It has been shown that the mixed-dimer model can explain the measured surface core-level shifts [12], STM images [11, 68] as well as the surface optical properties of the In-rich InP surface [14, 64, 71]. This has also been confirmed by independent computational studies [9, 10, 72]. Recently, an alternative mixed-dimer model was suggested on the basis of STM images [73]. Its total energy, however, is 0.34 eV per surface atom higher than that of the $\alpha 2(2 \times 4)$ geometry, which has the same stoichiometry.

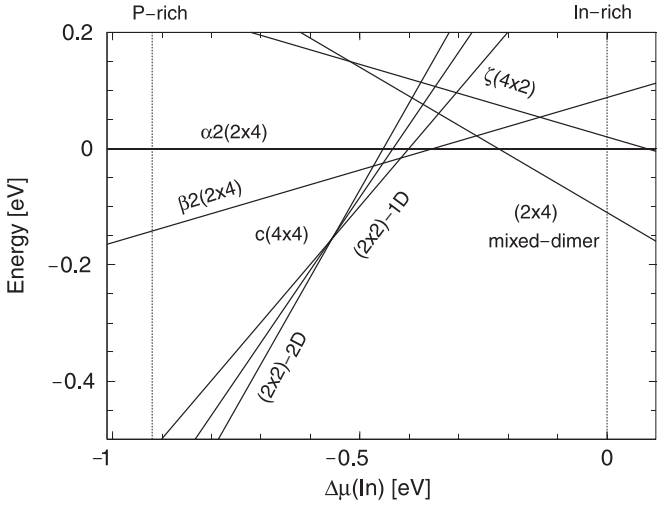

Fig. 3. Relative formation energy per (1×1) unit cell for InP surface reconstructions vs. the cation chemical potential. *Dashed lines* mark the approximate anion- and cation-rich limits of the thermodynamically allowed range of $\Delta\mu$ (In)

A reduction of the number of [110]-oriented cation–cation bonds, together with the formation of P−P dimers parallel to $[1\bar{1}0]$, occurs for the $\alpha 2(2 \times 4)$ and $\beta 2(2 \times 4)$ geometries predicted by theory for stoichiometric and slightly P-rich surfaces. This is in excellent accord with the evolution of the corresponding optical fingerprints [14, 54, 57, 58, 62] as demonstrated in [39, 71]. Thus it seems likely that the P-dimer models $\alpha 2$ and $\beta 2$ represent indeed the surface ground state as the P content increases. As a transitional state the formation of single P dimers on top of a complete In layer underneath has been suggested on the basis of STM results [60].

A detailed account of the surface electronic properties of InP (001)(2×4) may be found in [55, 64, 65, 68].

The reconstructions formed for P content higher than that characteristic for (2×4) surfaces are not fully understood. Li et al. [60, 69] observed by STM the formation of buckled P dimers, giving rise to $p(2 \times 2)$ and $c(4 \times 2)$ domains for the nominal (2×1) reconstructed P-rich surface. They assume these P dimers to be formed on top of the In-terminated substrate. In order to explain the semiconducting nature of the surface, they speculate that an electron pairing across the dimer rows occurs. Similar structures were suggested by Vogt et al. on the basis of STM results [70] and core-level measurements [66]. Pulci et al. studied the suggested geometries by ab initio total-energy calculations and found them unstable with respect to the formation of P dimers on top of a P-terminated substrate [74]. Such structures are seemingly observed by STM for surfaces with an even higher P content [60, 70]. La-Bella et al. report similar STM pictures [59]. In addition, however, they found $c(4 \times 4)$ reconstructed domains, which are reminiscent of the GaAs (001)$c(4 \times 4)$ surface, characterised by three anion dimers on top of an anion-terminated substrate. Ozanyan et al. [75], who also observe a P-rich $c(4 \times 4)$ reconstructed InP surface, on the other hand conclude from the optical signature of the surface a geometry different from the one known from GaAs (001)$c(4 \times 4)$. In [39] a number of $c(4 \times 4)$ surface reconstruction models, including the proposal by Ozanyan et al., were probed by total-energy calculations. It turned out that the three-dimer model known from GaAs (001)$c(4 \times 4)$ is the most favoured geometry also for InP.

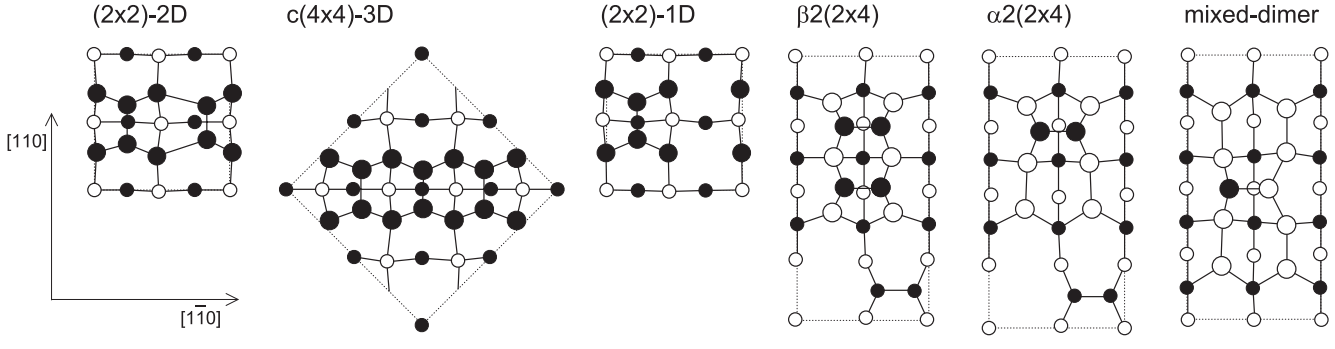

Fig. 4. Top view of relaxed InP (001) surface structures, ordered according to the In coverage. *Empty* (*filled*) *circles* represent In (P) atoms. Positions in the uppermost two atomic layers are indicated by *larger symbols*

All studies agree on the low long-range order and high density of defects of the P-rich surfaces. That may be understood from the calculated surface phase diagram in Fig. 3: the (2×2)-1D, $c(4\times4)$ and (2×2)-2D structures are nearly degenerate in energy.

Neither the (2×2)-1D nor the (2×2)-2D structure fulfill the electron-counting rule, since not all anion dangling bonds can be completely filled. Both structures, however, are semiconducting. This is due to the buckling of the dimers in the case of the (2×2)-1D surface. The two dimers of the (2×2)-2D structure, on the other hand, are geometrically and electronically inequivalent, thus opening a band gap. A detailed discussion of their surface electronic structure and simulated STM images are given in [74].

The failure of the calculations to account for all experimental findings of P-rich InP surfaces, in particular their failure to reproduce the zigzag chains observed on MOVPE-grown surfaces [60, 66, 69, 70], which are seemingly formed by buckled P dimers, may be related to the presence of adsorbates such as hydrogen. This hypothesis is particularly plausible since only MOVPE-grown surfaces seem to feature such zigzag chains. The $c(4\times4)$ symmetry, on the other hand, appears to be observable only for MBE-grown samples [59, 75].

2.3 GaAs

The GaAs (001) surface is known to exhibit a very rich variety of ordered phases whose occurrence depends on the preparation conditions (see e.g. [1, 3]). Among them, the As-rich (2×4) reconstructions were extensively investigated in the past, due to their importance for the MBE growth of GaAs. Farrel and Palmstrøm [76] correlated, in their reflection high-energy electron diffraction (RHEED) study, characteristic patterns with the surface stoichiometry and distinguished between three (2×4) phases, called α, β and γ.

The α phase occurs at the highest substrate temperature and was suggested to correspond to a geometry combining two As dimers in the uppermost atomic layer with Ga−Ga bonds in the layer underneath. Schmidt et al. showed recently that the same stoichiometry can be realised with an energetically more favoured structure, called $\alpha2(2\times4)$ [7]. This structure, shown in Fig. 5, is 0.034 eV per (1×1) unit cell lower in energy than the α model. As both structures have the same stoichiometry, there is no dependence on the chemical potentials of the surface constituents. The α structure will be unstable with respect to α2 irrespective of the surface-preparation conditions. That result is somewhat surprising, as the α model is seemingly well-established [3]. Its geometry has mainly been concluded from filled-state STM images, showing two 'humps' along the [110] direction in each unit cell, which were interpreted as As dangling bonds [77–79]. This interpretation is plausible, but not necessarily imperative, as the second-layer Ga−Ga bonds of the α2 model will show up in filled-state STM images close to the positions of the assumed As atoms. The InP (001) surface provides a recent example for a misinterpretation of cation–cation bonds as anion dangling bonds [11, 68]. Of particular interest in that respect is the observation by Broekman et al. [79] of a slight asymmetry of the anion dimers of the α phase. The α geometry, possessing mirror symmetry, can hardly explain such a finding. The third-layer As dimer of the α2 structure, however, induces a slight buckling of the upper As dimer of about 0.02 Å. The reflectance anisotropy spectrum of the α phase of GaAs (001) [80] indicates a coexistence of anion dimers oriented along the $[\bar{1}10]$ direction with cation–cation bonds parallel to [110]. These features are present, however, also for the $\alpha2(2\times4)$ geometry: the calculated bond lengths amount to 2.47 and 2.50 Å for the uppermost and third-layer As dimers, respectively. The Ga−Ga bond length in the second atomic layer is 2.49 Å. It remains to be seen whether the α2 structure can account for the RHEED spot intensities assigned to the α phase of GaAs (001) [77, 78].

The bonding configuration of the α2 structure is very similar to the one of the α model [81]. Both structures comply with electron-counting heuristics. They differ, however, in their electrostatics. Since the anion dimer bond accommodates six electrons [82] in addition to the eight electrons forming the four bonds to the substrate, one expects a Coulomb repulsion between the negatively charged dimers. The surface may lower its electrostatic energy by distributing the dimers as uniformly as possible. Northrup and Froyen [6] suggested assigning point charges to the surface atoms according to the electron-counting rule, in order to estimate the Coulomb con-

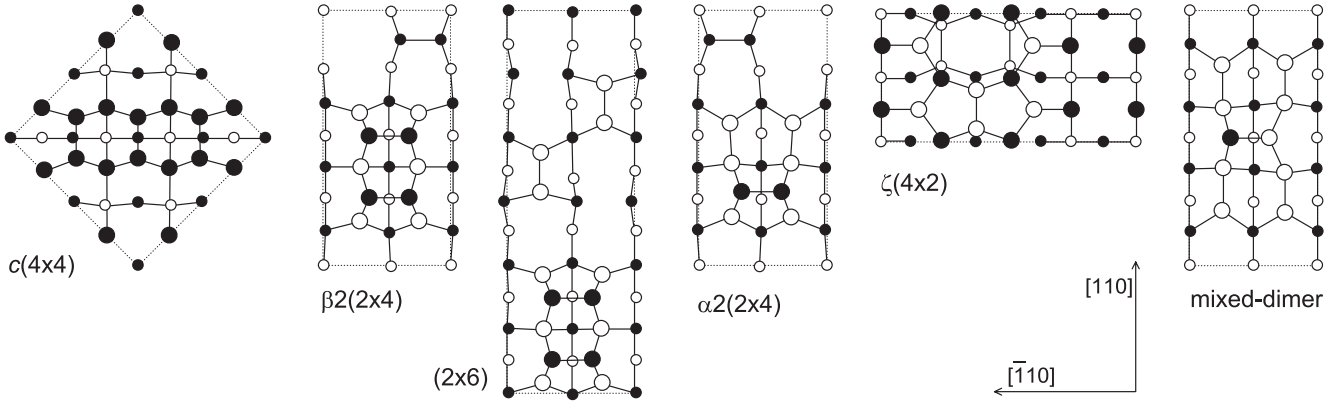

Fig. 5. Top view of relaxed GaAs (001) surface structures, ordered according to the Ga coverage. *Empty* (*filled*) *circles* represent Ga (As) atoms. Positions in the uppermost two atomic layers are indicated by *larger symbols*

tribution to the energy difference between surface structures. Based on such a charge distribution, one can then perform a Madelung summation for a periodic lattice of point charges,

$$S = \frac{1}{2} \sum_{i,j} \frac{q_i q_j}{|\boldsymbol{r}_i - \boldsymbol{r}_j|} ,$$

where the vectors $\boldsymbol{r}_i$ are the positions of the atoms which have been assigned charge q_i. The screening can be approximated by dividing S by the static dielectric constant of GaAs ($\varepsilon \sim 13$). That rough estimate yields a difference in electrostatic energies between α and α2 of 0.038 eV per (1×1) surface unit cell. That is remarkably close to the energy difference of 0.034 eV obtained from first principles. The quantitative agreement is fortuitous: the concept of homogeneously screened point charges is only a crude approximation. Nevertheless, it shows that the α2 structure is indeed stabilised with respect to α by its more favourable electrostatics. The actual occurrence of the predicted structure, however, remains to be proven experimentally.

The β phase, which is stable for more anion-rich conditions, was explained originally by the three-dimer model due to Chadi [83]. Northrup and Froyen [6] later showed that a somewhat modified structure, called β2 (Fig. 5), leads to a lower electrostatic energy and is energetically favoured. Other total-energy calculations [81, 82, 84] confirmed this result. The actual occurrence of the $\beta2(2 \times 4)$ structure was proven by in situ grazing incidence X-ray-diffraction measurements [85], dynamical RHEED analysis [86] and very recently by highly resolved STM images [87]. Details of the electronic structure of GaAs (001)$\beta2(2 \times 4)$ are given in [82].

The γ phase, finally, occurring for even more As-rich surfaces, was found to be a mixture of the β phase and the $c(4 \times 4)$ phase, with the surface As coverage varying depending on the actual growth conditions [77, 78]. Moll et al. [84] performed total-energy calculations for several $c(4 \times 4)$ structures. In agreement with the present study, they find the three-dimer structure due to Sauvage-Simkin et al. [88] to have the lowest energy (cf. Fig. 5). Recently, a detailed discussion of the electronic properties of the $c(4 \times 4)$ reconstructed GaAs (001) surface has been published [89].

The Ga-rich GaAs (001)(4×2) reconstruction has not been studied as extensively. Biegelsen et al. [90] interpreted their STM images in terms of the $\beta2(4 \times 2)$ structure featuring three Ga dimers. This structure has also been supported by Xue et al. [91], based on STM. No confirmation of that structural model by an independent experimental technique, however, could be obtained. Moreover, Skala et al. [92] suggested a radically different As-dimer structure to explain STM images of the (4×2) reconstructed GaAs surface. A further geometry, called $\beta3(4 \times 2)$ in accordance with the generally accepted nomenclature for GaAs (001) surfaces, was suggested by Moriarty et al. [93] to account for their STM results. Finally, a three-Ga-dimer model has been concluded from a low-energy electron-diffraction (LEED) analysis [94] of the Ga-rich GaAs (001)(4×2) surface. The three-Ga-dimer model as well as the (4×2) As-dimer structure were found unstable in ab initio total-energy calculations, however [6, 84]. Instead, total-energy calculations prompted Lee et al. [17] to suggest a rather complex, so-called ζ structure, for the Ga-rich GaAs $(001)(4 \times 2)/c(8 \times 2)$ surfaces. The stability of the ζ structure with respect to all previously suggested (4×2) geometries was confirmed by the present author and others in [7, 95].

The ζ structure, shown in Fig. 6, contains two Ga dimers in the second atomic layer and one Ga dimer as well as threefold-coordinated Ga and As atoms in the topmost layer. It has the same stoichiometry as the $\beta2(4 \times 2)$ model. Its higher stability has been traced back to its more favorable electrostatics. In view of the complexity of the ζ model it might be thought that other structures, containing similarly complex structural elements, could as well describe the Ga-rich GaAs surface. Lee et al. show, however, that the STM images simulated for the proposed structure are in good accord with the experimental data. Also, a LEED analysis [17] as well as X-ray-diffraction data [96, 97] lend further credibility to the newly proposed model. The calculated phase diagram for GaAs (001) in Fig. 7 indicates that for extreme Ga-rich conditions the $\zeta(4 \times 2)$ surface should transform into a (2×4) reconstructed mixed-dimer structure. Such a phase

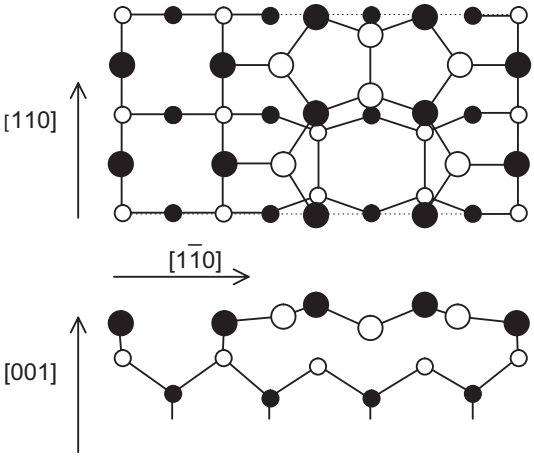

Fig. 6. Top view and side view of the relaxed GaAs (001)ζ(4×2) surface structure. *Empty* (*filled*) *circles* represent Ga (As) atoms

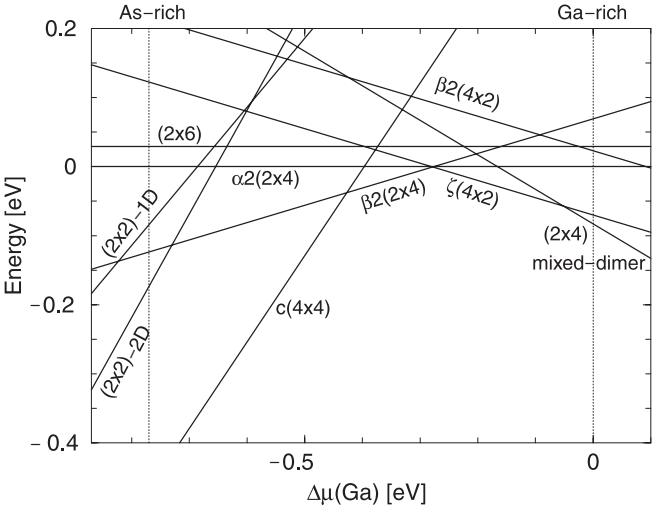

Fig. 7. Relative formation energy per (1×1) unit cell for GaAs surface reconstructions vs. the cation chemical potential. *Dashed lines* mark the approximate anion- and cation-rich limits of the thermodynamically allowed range of $\Delta\mu$ (Ga)

transition is not observed experimentally. Rather a (4×6) surface forms, which will be discussed below.

The calculated band structure of the $\zeta(4 \times 2)$ surface together with the orbital character of the relevant surface states is shown in Fig. 8.

The occupied surface states are energetically below the bulk valence-band maximum. The bound surface valence bands are derived from surface anion related orbitals. Interestingly, $V1$, the highest surface state, is rather delocalised with the probability maximum in the third atomic layer. $V2$, $V3$ and $V4$ are localised at the first-layer anions forming the bridge between first and second atomic layers. These states appear most prominent in filled-state STM images at low bias [17] and were originally interpreted as fingerprints of the second-layer anions of the $\beta 2(4 \times 2)$ surface [98]. The bands derived from unoccupied surface states are pushed above the bulk conduction-band minimum. $C1$ and $C3$ are derived from empty Ga dimer states in the topmost layer. $C2$ is an antibonding state located between the third-layer anions and the second-layer Ga-dimer atoms. $C4$ comprises both anion and cation empty dangling bonds in the topmost atomic layer.

When discussing the band structure in Fig. 8, a word of caution is in order. The presented band structure suffers from the well-known DFT–LDA-gap problem, i.e. the underestimation of the excitation energies [99, 100]. The inclusion of electronic self-energy effects may lead to different energy shifts for bulk and surface state energies, as demonstrated for GaP (001) and InP (001) surfaces in [41, 64]. Experience shows, however, that the relative ordering and orbital character of the surface states are usually reliably described within DFT–LDA.

Structural models were also proposed for GaAs (001) surface reconstructions larger than (2×4) or (4×2). A (1×6) symmetry was observed by electron diffraction [3] as a non-equilibrium or transient phase between As- and Ga-rich surfaces. STM images by Biegelsen et al. [90] and Kuball et al. [4] revealed that (2×6) and (6×6) reconstructed domains are responsible for the observed LEED patterns. The energy of Biegelsen's model for the (2×6) surface has been approximated by a linear combination of structural motifs (LCSMs) method by Zhang and Zunger [8]. They found it to be higher in energy than the $\alpha(2 \times 4)$ structure by 0.034 eV per (1×1) surface unit cell. More precise ab initio calculations [95] indicate that the energy difference is actually much smaller, 0.006 eV. By a simple rearrangement of the As dimers in blocks instead of zigzag chains, resulting in the (2×6) structure shown in Fig. 5, a further lowering of the surface energy below the value of the $\alpha(2 \times 4)$ structure is possible [95]. Still, the energy gain is not sufficient to make this (2×6) geometry more favourable than the newly proposed $\alpha 2(2 \times 4)$ structure (see calculated phase diagram in Fig. 7). The surface energy of the (6×6) model suggested in [4] will very likely be in the same range as the one calculated for the (2×6) reconstruction, as the models are rather similar. The stability of the stoichiometric $\alpha 2(2 \times 4)$ surface is limited to a very small window of preparation conditions, as can be seen from Fig. 7. Given the higher energy of the (2×6) and probably also the (6×6) surface, these structures are only metastable. This may explain their low long-range order.

The GaAs (001)(4×6) surface is another large reconstruction that is extensively discussed in the literature (see [3] for a comprehensive review). Xue et al. point out that one has to discriminate between a genuine (4×6) reconstruction, which is more Ga-rich than the Ga-rich (4×2) reconstruction, and a pseudo (4×6) phase, which actually consists of a mixture of the (1×6), the (4×2) and the genuine (4×6) phase. To explain the surface structure of the genuine GaAs (001)(4×6) surface, Xue et al. [3, 91] propose a regular array of Ga clusters containing six to eight atoms on top of a (4×2) reconstructed GaAs surface (see Fig. 9). The concept of 'magic' numbers of electrons in free metal clusters allows an initial guess of the size of stable Ga clusters. Both experiment and model calculations indicate that clusters of simple, monovalent metals are particularly stable if they contain a so-called magic number of electrons such as 8, 20, 40, ... [101, 102]. In the present case, of course, the number of electrons in the cluster is modified by the charge transfer from the substrate [103]. If one assumes the cluster to be bonded to four

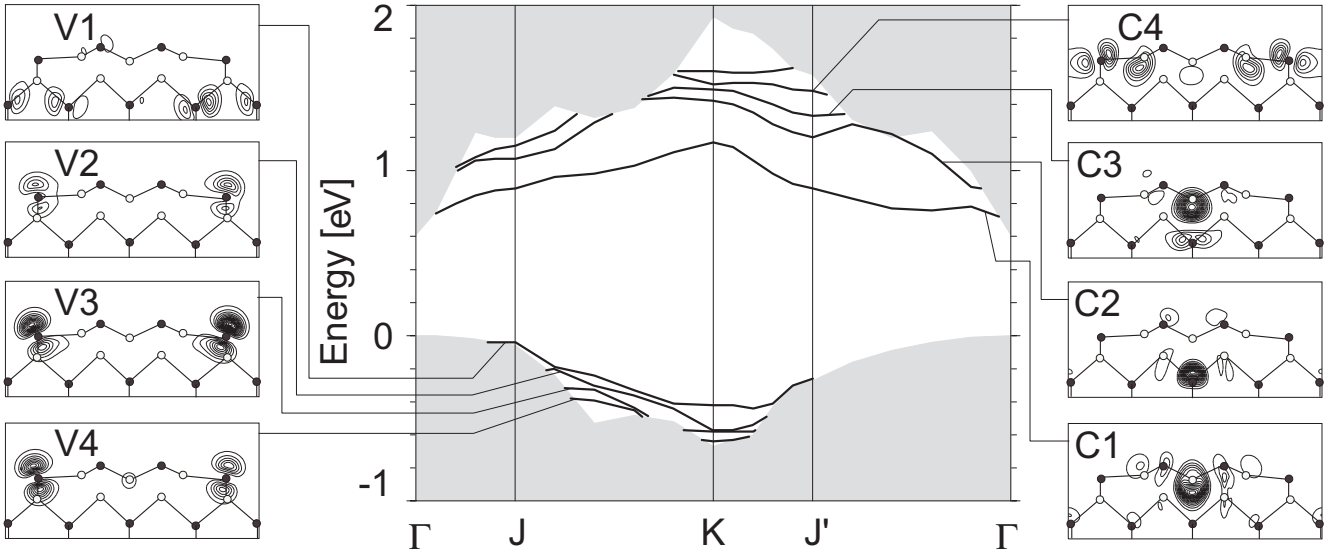

Fig. 8. Surface band structure (bound states) for the GaAs (001)$\zeta(4 \times 2)$ surface. *Grey regions* indicate the projected bulk band structure. *Left* and *right*: the corresponding squared wave functions at K. The contour spacing is $\frac{1}{3} \times 10^{-3}$ Bohr^{-3}

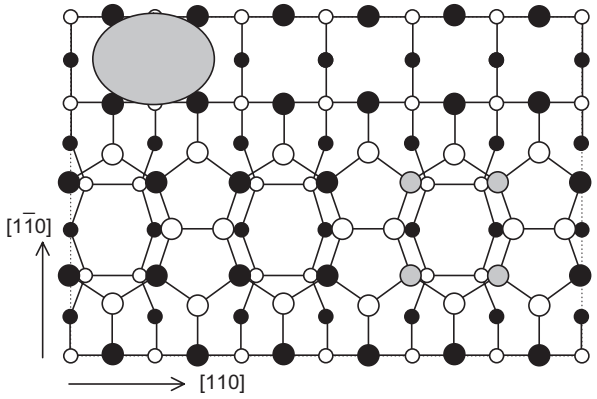

Fig. 9. Top view of investigated GaAs (001)(4×6) surface. *Empty* (*filled*) *circles* represent Ga (As) atoms. Positions in the uppermost two atomic layers are indicated by *larger symbols*. The *large oval shape* indicates trial Ga clusters. Positions of surface anions which were substituted by Ga in the substitution models are filled in *grey*

surface anions as indicated in Fig. 9, each anion donating the electrons from its originally doubly-occupied dangling bond into the cluster, a minimum stable metal cluster containing 20 electrons would consist of four gallium atoms. In the present work a number of adsorbed clusters ranging in size from four to eight atoms ($C4$, ..., $C8$) with a variety of shapes and orientations were studied by means of first-principles total-energy calculations. The adsorption energies of the most favourable configuration for each cluster size are compiled in Table 1. All investigated cluster geometries are higher in energy than the Ga-rich GaAs (001)ζ(4×2) surface even at the most Ga-rich conditions, where the Ga chemical potential assumes its bulk value. Unless a specific cluster configuration has been missed, the structural model proposed by Xue et al. is thus not borne out by the ab initio calculations. Moreover, considering the trend in the surface energies, no indication for the energetic preference of a certain magic cluster size can be recognised. Instead, the larger the clusters become, the more unfavourable their adsorption seems to be.

Table 1. Relative surface energies for single adatoms ($C1$), addimers ($C2$), adsorbed Ga cluster configurations ($C4, \ldots, C8$) as well as for substitutional models ($S1$ and $S4$) forming (4×6) reconstructions. The energies refer to a (1×1) surface unit cell and are given with respect the Ga-rich GaAs (001)ζ(4×2) surface under extreme Ga-rich conditions ($\mu(\mathrm{Ga}) = \mu(\mathrm{Ga})_{\mathrm{bulk}}$)

Structure	$C1$	$C2$	$C4$	$C5$	$C6$	$C8$	$S1$	$S4$
ΔE (meV)	28	48	119	161	153	225	29	121

I also probed the adsorption of single, fourfold-coordinated Ga adatoms as suggested by Kumpf et al. [97] ($C1$) as well as the formation of Ga addimers ($C2$) at the position indicated by the grey oval shape in Fig. 9. However, these adstructures are only metastable, as shown in Table 1. As an alternative geometry the substitution of one ($S1$) or four ($S4$) of the surface anions marked grey in Fig. 9 by Ga atoms was investigated. The substitutional sites are three-fold-coordinated and should therefore be favoured by sp^2-like bonded group-III atoms. Nevertheless, the two surface structures considered are higher in energy than the GaAs (001)ζ(4×2) surface.

Recently, a very different interpretation of what appears to be Ga clusters in the STM images of (4×6) surfaces has been given. Kruse et al. [104] showed that the bright spots disappear upon chemical titration with just 7.5×10^{-4} monolayers of O_2. The spots also do not show up when empty states are imaged. This led Kruse et al. to conclude that the bright spots arise from surface excess charge localised in the gallium dangling bonds. Repulsion between the trapped negative charge leads to what appears to be a surface reconstruction. That hypothesis is very interesting but rather speculative. The geometry of the (4×6) reconstructed GaAs (001) surface thus remains an open question.

2.4 InAs

The surface phase diagram of InAs (001), while less investigated, appears to be similar to the one of GaAs. (4×2), (2×4) [105–110] and $c(4 \times 4)$ reconstructions [111] are observed with increasing surface As content. STM images of (2×4) reconstructed InAs surfaces [107, 112] are interpreted in terms of the β2(2×4) geometry (cf. Fig. 10) for the more As-rich case, while a α2(2×4) structure seems to form after annealing. This picture is supported by first-principles total-energy calculations [112, 113]. The existence of the β2(2×4) structure was also confirmed by X-ray-diffraction experiments [109]. Miwa and Srivastava [113] recently published a very comprehensive study of the geometrical and electronic properties of InAs (001)(2×4) surfaces.

Less clear is the structure of the In-rich (4×2) surface. A β3(4×2) geometry was proposed on the basis of STM

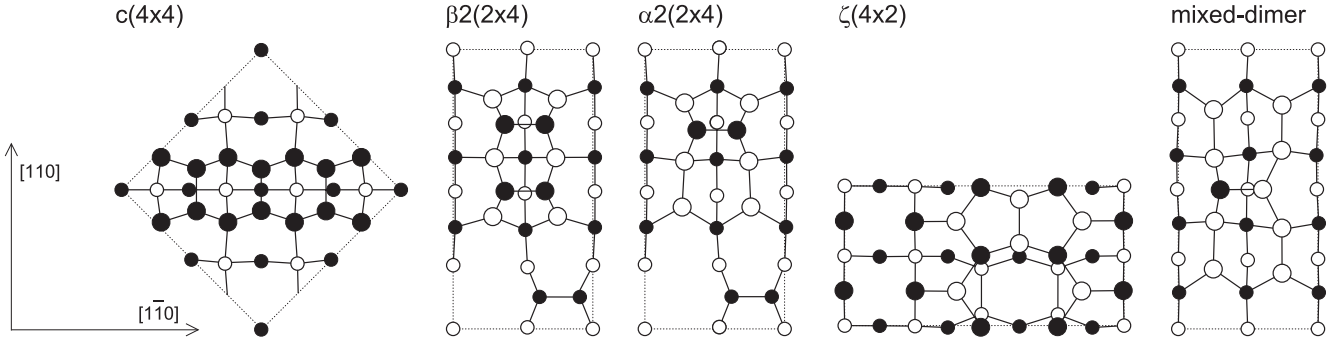

Fig. 10. Top view of relaxed InAs (001) surface structures, ordered according to the In coverage. *Empty* (*filled*) *circles* represent In (As) atoms. Positions in the uppermost two atomic layers are indicated by *larger symbols*

images [106], while total-energy calculations by Ratsch et al. [112] failed to find a stable (4×2) surface.

In the present study the $\zeta(4 \times 2)$ structure suggested by Lee et al. [17] for Ga-rich GaAs surfaces was probed for InAs (001). It indeed turns out to be energetically stable for a certain window of In-rich surface-preparation conditions, as shown in the calculated phase diagram in Fig. 11. Also, a very recent X-ray-diffraction analysis of $c(8 \times 2)$ reconstructed InAs (001) indicates a ζ-like geometry [97]. Therefore, it seems that the ζ structure solves the structural puzzle of the In-rich InAs (001)(4×2) surface.

For extreme In-rich conditions the calculations predict a change of reconstruction again. A (2×4) mixed-dimer structure should then be favoured. Such a second phase transition is not observed experimentally. The theoretical finding may well be an artefact of the limited accuracy in the calculation of the surface phase diagram, in particular with respect to the boundaries of the thermodynamically allowed region [25]. Also, the occurrence of a modified, even more In-rich $\zeta(4 \times 2)$ structure, for example the adsorption of additional cations as suggested in [97], would explain the apparent contradiction.

For As-rich surfaces, finally, the three-dimer $c(4 \times 4)$ structure known from GaAs has the lowest energy.

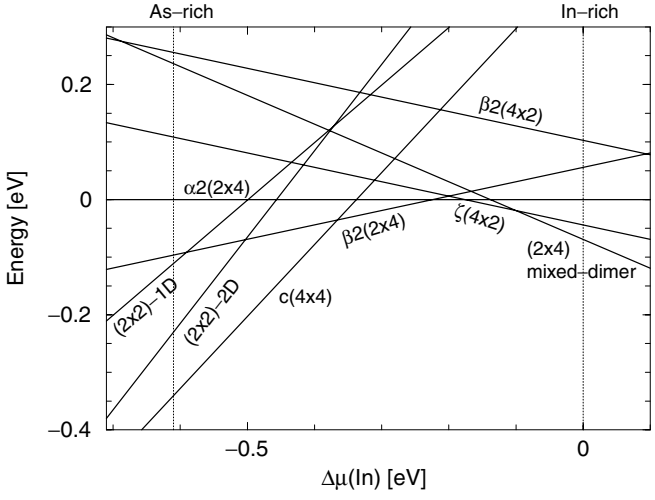

Fig. 11. Relative formation energy per (1×1) unit cell for InAs surface reconstructions vs. the cation chemical potential. *Dashed lines* mark the approximate anion- and cation-rich limits of the thermodynamically allowed range of $\Delta\mu$ (In)

2.5 Chemical trend

Nowadays the calculation of accurate surface energies from first principles has become feasible even for relatively large systems. Powerful supercomputers like the Cray T3E or the Hitachi SR8000-F1 running massively parallel codes such as the one developed in the Bernholc group [23, 114] allow us to calculate surface energies for typical (2×4) reconstructions within a few minutes. Even ground-state energies for structures as large as the GaAs (001)(4×6) surfaces discussed above are obtained after only a couple of hours. Still, empirical concepts such as those discussed in the introduction are of high value. Only these concepts allow us to truly understand the mechanisms and driving forces behind the overwhelming variety of surface structures. Their predictions must be critically compared, however, to the experimental findings and computational results obtained from first principles.

The newly proposed GaAs (001)$\zeta(4\times2)$ is an excellent example in that respect. It features no less than eight anion dangling bonds per surface unit cell. According to Mirbt et al.'s theory of the surface-reconstruction parameter [9], this structure should never be stable in a cation-rich environment. Still, recent calculations including the present work clearly favour the structure, which is seemingly also in agreement with experiment [96, 97]. Even the very powerful concept of the electron-counting rule does not apply to all III−V (001) surfaces, as shown for P-rich InP surfaces, where (2×2) reconstructions may form.

Can the formation of geometrical models which defy commonly accepted surface-reconstruction principles be understood from simple arguments? A particular choice of the size difference between the surface anions and cations may be a likely explanation why specific surface geometries are favoured for specific materials. In Fig. 12 I have plotted the relative stabilities of the cation-rich $\zeta(4 \times 2)$ and the anion-rich (2×2)-2D surfaces vs. the relative difference between the covalent radii of the surface constituents for different materials. Obviously, the larger the size difference between surface cations and anions becomes, the more favourable is the (2×2)-2D structure. The reduction of surface stress releases more energy than can be gained by complying with the electron-counting rule. In that respect it is interesting to note that other III−V surfaces which are known to violate the ECR such as AlSb (001), GaSb (001) [16] and GaN (0001) [115] are as well characterised by largely different sizes of anions and cations. However, surface geometries which satisfy the electron counting rule, such as the $\zeta(4 \times 2)$ and the $\alpha2(2 \times 4)$ models, follow a distinct, albeit less pronounced trend with the geometrical inequivalence as can be seen from Fig. 12. The influence of stress on the surface reconstructions of III−V (001) surfaces has also been underlined in a recent ab initio study by Ratsch [116]. It seems as if, apart from electrostatics, covalent radii and bond lengths are still the

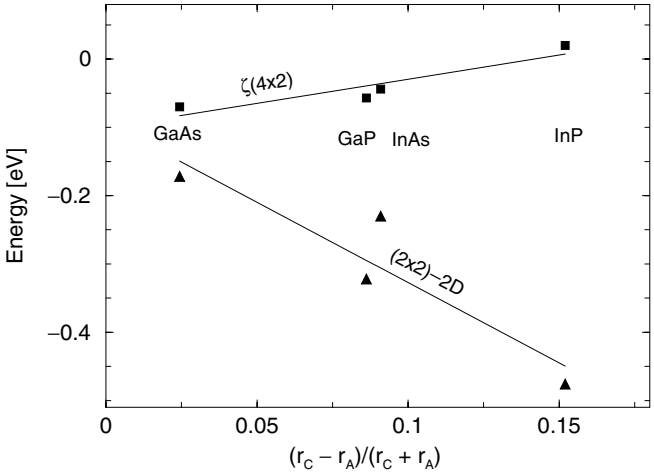

Fig. 12. Energy differences between the $\zeta(4 \times 2)/(2 \times 2)$-2D surface geometries and the stoichiometric $\alpha2(2 \times 4)$ surface for cation-rich/anion-rich conditions. The results are plotted vs. the relative size difference between surface cations and anions. *Solid lines* are to guide the eye

most reliable guides in predicting stable semiconductor surface structures.

3 Summary

A short review of the structure and stability of (001) surfaces of GaP, InP, GaAs and InAs has been presented. Experimental and earlier theoretical findings were compared with results of accurate total-energy calculations from first principles. The stabilities of surface geometries follow a distinct trend determined by the size ratio of the surface constituents. Most experimental results can be very well explained on the basis of the calculations. Some reconstruction models such as $\beta 2(2\times 4)$ and $\alpha 2(2\times 4)$ seem to occur for all considered materials for specific preparation conditions. Not all surface reconstructions, however, are presently understood. The anion-rich GaP and InP surfaces belong to this category. The apparent contradictions between theory and experiment concerning the structure of these surfaces may be related to the surface preparation. Calculations modelling the MOVPE process will hopefully be able to resolve the discrepancies. Open questions also remain concerning the cation-rich surfaces of GaAs and InAs. The Ga-rich GaAs $(001)(4\times 6)$ surface is a particularly interesting example in that respect.

Acknowledgements. I have benefited from discussions with many colleagues on this subject matter. In particular I want to thank F. Bechstedt, S. Mirbt and N. Esser. Grants of computer time from the Höchstleistungsrechenzentrum Stuttgart, the Leibniz-Rechenzentrum München and the John von Neumann-Institut Jülich are gratefully acknowledged.

References

1. L. Däweritz, R. Hey: Surf. Sci. **236**, 15 (1990)
2. W. Mönch: *Semiconductor Surfaces and Interfaces* (Springer, Berlin 1995)
3. Q.-K. Xue, T. Hashizume, T. Sakurai: Prog. Surf. Sci. **56**, 1 (1997)
4. M. Kuball, D.T. Wang, N. Esser, M. Cardona, J. Zegenhagen: Phys. Rev. B **51**, 13 880 (1995)
5. M.D. Pashley: Phys. Rev. B **40**, 10 481 (1989)
6. J.E. Northrup, S. Froyen: Phys. Rev. B **50**, 2015 (1994)
7. W.G. Schmidt, S. Mirbt, F. Bechstedt: Phys. Rev. B **62**, 8087 (2000)
8. S.B. Zhang, A. Zunger: Phys. Rev. B **53**, 1343 (1996)
9. S. Mirbt, N. Moll, A. Kley, J.D. Joannopoulos: Surf. Sci. **422**, L177 (1999)
10. S. Mirbt, N. Moll, K. Cho, J.D. Joannopoulos: Phys. Rev. B **60**, 13 283 (1999)
11. C.D. MacPherson, R.A. Wolkow, C.E.J. Mitchell, A.B. McLean: Phys. Rev. Lett. **77**, 691 (1996)
12. W.G. Schmidt, F. Bechstedt, N. Esser, M. Pristovsek, C. Schultz, W. Richter: Phys. Rev. B **57**, 14 596 (1998)
13. A.M. Frisch, W.G. Schmidt, J. Bernholc, M. Pristovsek, N. Esser, W. Richter: Phys. Rev. B **60**, 2488 (1999)
14. K.B. Ozanyan, P.J. Parbrook, M. Hopkinson, C.R. Whitehouse, Z. Sobiesierski, D.I. Westwood: J. Appl. Phys. **82**, 474 (1997)
15. I.M. Vitomirov, A. Raisanen, L.J. Brillson, C.L. Lin, D.T. McInturff, P.D. Kirchner, J.M. Woodall: J. Vac. Sci. Technol. A **11**, 841 (1993)
16. L.J. Whitman, P.M. Thibado, S.C. Erwin, B.R. Bennett, B.V. Shanabrook: Phys. Rev. Lett. **79**, 693 (1997)
17. S.-H. Lee, W. Moritz, M. Scheffler: Phys. Rev. Lett. **85**, 3890 (2000)
18. P. Hohenberg, W. Kohn: Phys. Rev. **136**, B864 (1964)
19. W. Kohn, L.J. Sham: Phys. Rev. **140**, A1133 (1965)
20. D.M. Ceperley, B.J. Alder: Phys. Rev. Lett. **45**, 566 (1980)
21. J.P. Perdew, A. Zunger: Phys. Rev. B **23**, 5048 (1981)
22. M. Fuchs, M. Scheffler: Comput. Phys. Commun. **119**, 67 (1999)
23. E.L. Briggs, D.J. Sullivan, J. Bernholc: Phys. Rev. B **54**, 14 362 (1996)
24. J.B. Mullin *et al.*, V.N. Bessolov *et al.*, J.V. Ozolin *et al.*, G. Giesecke *et al.*: in *Landolt-Börnstein, Numerical Data and Functional Relationships in Science and Technology*, Vol. III, ed. by O. Madelung (Springer, Berlin 1982) p. 17a
25. W.G. Schmidt: Appl. Phys. A **65**, 581 (1997)
26. J.N. Baillargeon, K.Y. Cheng, K.C. Hsieh: Appl. Phys. Lett. **56**, 2201 (1990)
27. N. Sanada, M. Shimonmura, Y. Fukuda, T. Sato: Appl. Phys. Lett. **67**, 1432 (1995)
28. A. Watanabe, H. Shimaya, N. Naitoh, S. Nishigaki: J. Vac. Sci. Technol. B **14**, 3599 (1996)
29. Y. Fukuda, M. Shimomura, N. Sanada: J. Appl. Phys. **76**, 3632 (1994)
30. M.M. Sung, J.W. Rabalais: Surf. Sci. **365**, 136 (1996)
31. M. Naitoh, A. Watanabe, A. Konishi, S. Nishigaki: Jpn. J. Appl. Phys. Part 1 **35**, 4789 (1996)
32. N. Oishi, F. Shoji, A. Konishi, M. Naitoh, S. Nishigaki: Surf. Rev. Lett. **5**, 223 (1998)
33. N. Sanada, S. Mochizuki, S. Ichikawa, N. Utsumi, M. Shimomura, G. Kaneda, A. Takeuchi, Y. Suzuki, Y. Fukuda, S. Tanaka, M. Kamata: Surf. Sci. **419**, 120 (1999)
34. M. Naitoh, A. Konishi, H. Inenaga, S. Nishigaki, N. Oishi, F. Shoji: Surf. Sci. **402–404**, 623 (1998)
35. M. Yoshikawa, A. Nakamura, T. Nomura, K. Ishikawa: Jpn. J. Appl. Phys. Part 1 **35**, 1205 (1996)
36. P.A. Postigo, G. Armelles, T. Utzmeier, F. Briones: Phys. Rev. B **57**, 1359 (1998)
37. M. Zorn, B. Junno, T. Trepk, S. Bose, L. Samuelson, J.-T. Zettler, W. Richter: Phys. Rev. B **60**, 11 557 (1999)
38. Y. Fukuda, N. Sekizawa, S. Mochizuki, S. Sanada: J. Cryst. Growth **221**, 26 (2000)
39. W.G. Schmidt, J. Bernholc, F. Bechstedt: Appl. Surf. Sci. **166**, 179 (2000)
40. O. Pulci, W.G. Schmidt, F. Bechstedt: Phys. Status Solidi A **184**, 105 (2001)
41. W.G. Schmidt, J.L. Fattebert, J. Bernholc, F. Bechstedt: Surf. Rev. Lett. **6**, 1159 (1999)
42. K. Lüdge, P. Vogt, O. Pulci, N. Esser, F. Bechstedt, W. Richter: Phys. Rev. B **62**, 11 046 (2000)
43. N. Kobayashi, Y. Kobayashi, K. Uwai: J. Cryst. Growth **170**, 225 (1997)
44. X. Wang: Appl. Surf. Sci. **33–34**, 88 (1988)
45. X. Hou, G. Dong, X. Ding, X. Wang: J. Phys. C: Solid State Phys. **20**, L121 (1987)
46. J.M. Moison, M. Bensoussan: Surf. Sci. **168**, 68 (1986)
47. W. Weiss, R. Hornstein, D. Schmeisser, W. Göpel: J. Vac. Sci. Technol. B **8**, 715 (1990)
48. J. Woll, T. Allinger, V. Polyakov, J.A. Schaefer, A. Goldmann, W. Erfurth: Surf. Sci. **315**, 293 (1994)
49. S. Riese, E. Milas, H. Merz: Surf. Sci. **270**, 833 (1992)
50. M.M. Sung, C. Kim, H. Bu, D.S. Karpuzov, J.W. Rabalais: Surf. Sci. **322**, 116 (1995)
51. M. Shimomura, N. Sanada, Y. Fukuda, P.J. Møller: Surf. Sci. **359**, L451 (1996)
52. B.X. Yang, H. Hasegawa: Jpn. J. Appl. Phys. **33**, 742 (1994)
53. N. Esser, U. Resch-Esser, M. Pristovsek, W. Richter: Phys. Rev. B **53**, R13 257 (1996)
54. D. Pahlke, J. Kinsky, C. Schultz, M. Pristovsek, M. Zorn, N. Esser, W. Richter: Phys. Rev. B **56**, R1661 (1997)
55. W.R.A. Huff, M. Shimomura, N. Sanada, G. Kaneda, T. Takeuchi, Y. Suzuki, H.W. Yeom, T. Abukawa, S. Kono, Y. Fukuda: Phys. Rev. B **57**, 10 132 (1998)
56. T.K. Johal, S.D. Barret, M. Hopkinson, P. Weightman, J.R. Power: J. Appl. Phys. **83**, 480 (1998)
57. J. Kinsky, C. Schultz, D. Pahlke, A.M. Frisch, T. Herrmann, N. Esser, W. Richter: Appl. Surf. Sci. **123–124**, 228 (1998)
58. M. Zorn, T. Trepk, J.-T. Zettler, B. Junno, C. Meyne, K. Knorr, T. Wethkamp, M. Klein, M. Miller, W. Richter, L. Samuelson: Appl. Phys. A **65**, 333 (1997)
59. V.P. LaBella, Z. Ding, D.W. Bullock, C. Emery, P.M. Thibado: J. Vac. Sci. Technol. A **18**, 1492 (2000)
60. L. Li, Q. Fu, C.H. Li, B.-K. Han, R.F. Hicks: Phys. Rev. B **61**, 10 223 (2000)
61. P.J. Parbrook, K.B. Ozanyan, M. Hopkinson, C.R. Whithouse, Z. Sobiesierski, D.I. Westwood: Appl. Surf. Sci. **123–124**, 313 (1998)

62. P.A. Postigo, G. Armelles, T. Utzmeier, F. Briones: Phys. Rev. B **57**, 1362 (1998)
63. M. Shimomura, N. Sanada, G. Kaneda, T. Takeuchi, Y. Suzuki, Y. Fukuda, W.R.A. Huff, T. Abukawa, S. Kono, H.W. Yeom, A. Kakizaki: Surf. Sci. **412–413**, 625 (1998)
64. W.G. Schmidt, N. Esser, A.M. Frisch, P. Vogt, J. Bernholc, F. Bechstedt, M. Zorn, T. Hannappel, S. Visbeck, F. Willig, W. Richter: Phys. Rev. B **61**, R16 335 (2000)
65. A.M. Frisch, P. Vogt, S. Visbeck, T. Hannappel, F. Willig, W. Braun, W. Richter, J. Bernholc, W.G. Schmidt, N. Esser: Appl. Surf. Sci. **166**, 224 (2000)
66. P. Vogt, A.M. Frisch, T. Hannappel, S. Visbeck, F. Willig, C. Jung, R. Follath, W. Braun, W. Richter, N. Esser: Appl. Surf. Sci. **166**, 190 (2000)
67. T. Hannappel, L. Toben, S. Visbeck, H.J. Crawack, C. Pettenkofer, F. Willig: Surf. Sci. **470**, L1 (2000)
68. W.G. Schmidt, F. Bechstedt: Surf. Sci. **409**, 474 (1998)
69. L. Li, B.-K. Han, Q. Fu, R.F. Hicks: Phys. Rev. Lett. **82**, 1879 (1999)
70. P. Vogt, T. Hannappel, S. Visbeck, K. Knorr, N. Esser, W. Richter: Phys. Rev. B **60**, R5117 (1999)
71. W.G. Schmidt, E.L. Briggs, J. Bernholc, F. Bechstedt: Phys. Rev. B **59**, 2234 (1999)
72. Q.K.K. Liu, N. Moll, M. Scheffler, E. Pehlke: Phys. Rev. B **60**, 17 008 (1999)
73. Q. Guo, M.E. Pemble, E.M. Williams: Surf. Sci. **468**, 92 (2000)
74. O. Pulci, K. Lüdge, W.G. Schmidt, F. Bechstedt: Surf. Sci. **464**, 272 (2000)
75. K.B. Ozanyan, P.J. Parbrook, M. Hopkinson, C.R. Whitehouse: In: Proceedings of the 24th International Conference on the Physics of Semiconductors (World Scientific, Singapore 1998) published on CD-ROM (ISBN 981-02-4030-9)
76. H.H. Farrel, C.J. Palmstrøm: J. Vac. Sci. Technol. B **8**, 903 (1990)
77. T. Hashizume, Q.-K. Xue, A. Ichimiya, T. Sakurai: Phys. Rev. Lett. **73**, 2208 (1995)
78. T. Hashizume, Q.-K. Xue, A. Ichimiya, T. Sakurai: Phys. Rev. B **51**, 4200 (1995)
79. L.D. Broekman, R.C.G. Leckey, J.D. Riley, A. Stampfl, B.F. Usher, B.A. Sexton: Phys. Rev. B **51**, 17 795 (1995)
80. A.I. Shkrebtii, N. Esser, W. Richter, W.G. Schmidt, F. Bechstedt, B.O. Fimland, A. Kley, R. Del Sole: Phys. Rev. Lett. **81**, 721 (1998)
81. W.G. Schmidt, F. Bechstedt: Surf. Sci. **360**, L473 (1996)
82. W.G. Schmidt, F. Bechstedt: Phys. Rev. B **54**, 16 742 (1996)
83. D.J. Chadi: J. Vac. Sci. Technol. A **5**, 834 (1987)
84. N. Moll, A. Kley, E. Pehlke, M. Scheffler: Phys. Rev. B **54**, 8844 (1996)
85. Y. Garreau, M. Sauvage-Simkin, N. Jedrecy, R. Pinchaux, M.B. Veron: Phys. Rev. B **54**, 17 638 (1996)
86. J.M. McCoy, U. Korte, P.A. Maksym: Surf. Sci. **418**, 273 (1998)
87. V.P. LaBella, H. Yang, D.W. Bullock, P.M. Thibado, P. Kratzer, M. Scheffler: Phys. Rev. Lett. **83**, 2989 (1999)
88. M. Sauvage-Simkin, R. Pinchaux, J. Massies, P. Calverie, N. Jedrecy, J. Bonnet, I.K. Robinson: Phys. Rev. Lett. **62**, 563 (1989)
89. T. Strasser, C. Solterbeck, W. Schattke, I. Bartoš, M. Cukr, P. Jiříček: Phys. Rev. B **63**, 5409 (2001)
90. D.K. Biegelsen, R.D. Bringans, J.E. Northrup, L.E. Swartz: Phys. Rev. B **41**, 5701 (1990)
91. Q.-K. Xue, T. Hashizume, J.M. Zhou, T. Sakata, T. Ohno, T. Sakurai: Phys. Rev. Lett. **74**, 3177 (1995)
92. S.L. Skala, J.S. Hubacek, J.R. Tucker, J.W. Lyding, S.T. Chou, K.-Y. Cheng: Phys. Rev. B **48**, 9138 (1993)
93. P. Moriarty, P.H. Beton, Y.-R. Ma, A.W. Dunn, M. Henini, D.A. Woolf: J. Vac. Sci. Technol. B **14**, 943 (1996)
94. J. Cérda, F.J. Palomares, F. Soria: Phys. Rev. Lett. **75**, 665 (1995)
95. W.G. Schmidt, S. Mirbt, F. Bechstedt: In: Proceedings of the 25th International Conference on the Physics of Semiconductors (Springer, Berlin 2001) p. 279
96. D. Paget, Y. Garreau, M. Sauvage, P. Chiaradia, R. Pinchaux, W.G. Schmidt: Phys. Rev. B **64**, R161 305 (2001)
97. C. Kumpf, L.D. Marks, D. Ellis, D. Smilgies, E. Landemark, M. Nielsen, R. Feidenhans'l, J. Zegenhagen, O. Bunk, J.H. Zeysing, Y. Su, R.L. Johnson: Phys. Rev. Lett. **86**, 3586 (2001)
98. T. Ohno: Surf. Sci. **357–358**, 265 (1996)
99. F. Bechstedt: in *Festköperprobleme/Advances in Solid State Physics*, Vol. 32, ed. by U. Rössler (Vieweg, Braunschweig/Wiesbaden 1992) p. 161
100. F. Aryasetiawan, O. Gunnarsson: Rep. Prog. Phys. **61**, 237 (1998)
101. W.A. de Heer: Rev. Mod. Phys. **65**, 611 (1993)
102. M. Brack: Rev. Mod. Phys. **65**, 677 (1993)
103. S. Tsukamoto, N. Koguchi: J. Cryst. Growth **209**, 258 (2000)
104. P. Kruse, J.G. McLean, A.C. Kummel: J. Chem. Phys. **113**, 2060 (2000)
105. H. Yamaguchi, Y. Horikoshi: Phys. Rev. B **45**, 1511 (1992)
106. S. Ohkouchi, N. Ikoma: Jpn. J. Appl. Phys. **33**, 3710 (1994)
107. H. Yamaguchi, Y. Horikoshi: Phys. Rev. B **51**, 9836 (1995)
108. B. Junno, S. Jeppesen, M.S. Miller, L. Samuelson: J. Cryst. Growth **164**, 66 (1996)
109. M. Göthelid, Y. Garreau, M. Sauvage-Simkin, R. Pinchaux, A. Cricenti, G.L. Lay: Phys. Rev. B **59**, 15 285 (1999)
110. V.L. Berkovits, N. Witkowski, Y. Borensztein, D. Paget: Phys. Rev. B **63**, R1314 (2001)
111. C. Ohler, C. Daniels, A. Forster, H. Lüth: J. Vac. Sci. Technol. B **15**, 702 (1997)
112. C. Ratsch, W. Barvoza-Carter, F. Grosse, J.H.G. Owen, J.J. Zinck: Phys. Rev. B **62**, R7719 (2000)
113. R.H. Miwa, G.P. Srivastava: Phys. Rev. B **62**, 15 778 (2000)
114. J. Bernholc, E.L. Briggs, C. Bungaro, M.B. Nardelli, J.L. Fattebert, K. Rapcewicz, C. Roland, W.G. Schmidt, Q. Zhao: Phys. Status Solidi B **217**, 685 (2000)
115. A.R. Smith, R.M. Feenstra, D.W. Greve, M.S. Shin, M. Skowronski, J. Neugebauer, J.E. Northrup: Surf. Sci. **423**, 70 (1999)
116. C. Ratsch: Phys. Rev. B **63**, R1306 (2001)